

Device Simulation of a Trench-IGBT with Integrated Diverter Structures

This article is based on the original paper "Trench-IGBTs with Integrated Diverter Structures" published by Rainer Constapel, Jacek Korec, and B. J. Baliga in Proceedings of ISPSD 95, Yokohama.

Introduction

This article illustrates the use of ATLAS in performing device design tasks for a Trench IGBT (TIGBT) structure. In conventional trench IGBTs the electric field at the corner of the trench can cause reliability problems. The ability of a device simulator to predict and enable user's to view the electric field distribution allow various device designs to be evaluated.

In this study a p⁺-diverter region is introduced at the bottom of the trench. This improves the reliability of the device by relaxing the electric field at the corner of the trench and diverts holes from entering the p-base region during forward conduction and switching. ATLAS was used to compare a structure with a diverter connected to the cathode either via a linear resistor or a pn-diode. Final analysis showed the diode diverter to be preferred. At 600V, the maximum field inside the oxide has been reduced from 1.4MV/cm to 0.1MV/cm. The most important result of the study was the excellent safe operating area of the proposed device.

Device Structure

The diverter is constructed by adding a p⁺-region and optionally a surrounding n-buffer under the trench gate region as illustrated in Figure 1. This additional doping can be performed by implanting Boron and Phosphorous into the bottom of the trench immediately after

etching it. The diverter is connected then to the cathode via a linear resistor or a nonlinear pn-diode, which drastically alters the electrical characteristic of the device.

The p⁺-region has several functions:

- It releases the electric field within the gate-oxide inside the corner of the trench. This should increase the reliability and long term stability of the device.
- It diverts holes from entering the p-base regions during forward conduction. This increases the latching current density, because a smaller fraction of the hole current flows into the p-base under the n⁺-source region, resulting in a larger forward biased safe operating area of the device.

The n-buffer surrounding the p⁺-region has the following function:

- During forward conduction, the channel current of the device flows around the p⁺-region resulting in a JFET pinch-off phenomenon between the p⁺-regions of neighboring IGBT-cells. Introducing the N buffer, the JFET-resistance should be minimized.

The proposed TIGBTs have been designed for a blocking voltage of about 600V and a threshold voltage of 4V. The essential geometrical and doping parameters were chosen to fit this spec. The device structure were formed using the graphical structure editor DevEdit. Analytical doping profiles were added to the device. DevEdit is able to produce meshes with no obtuse triangles based on the doping gradients and geometry of the structure. All simulations were performed using ATLAS/PISCES.

On-state Characteristics: Conventional TIGBT

Figure 2 shows the ATLAS result for the on-state voltage drop of a conventional TIGBT as a function of the cell-pitch for several fixed current densities.

The TIGBT show an excellent low on-state voltage drop, which decreases linearly in the observed cell-pitch range, indicating that for constant anode voltages the anode current density strongly increase with decreasing cell-pitch. The increase of the ratio of the channel

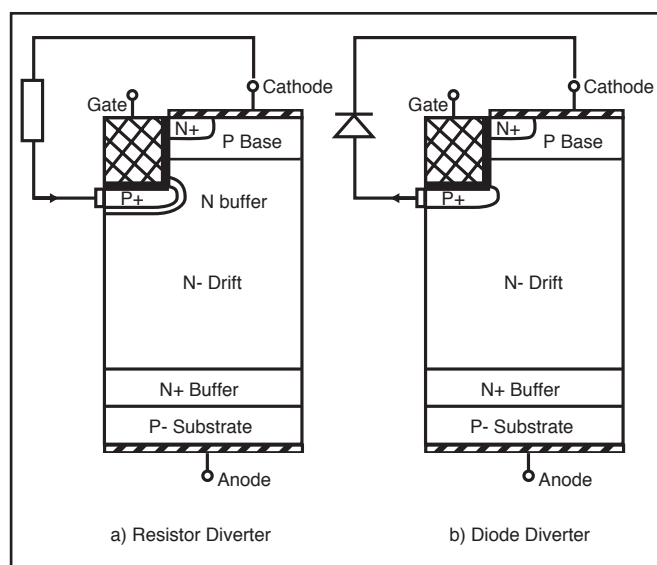


Figure 1. Trench IGBT with Integrated Diverter.

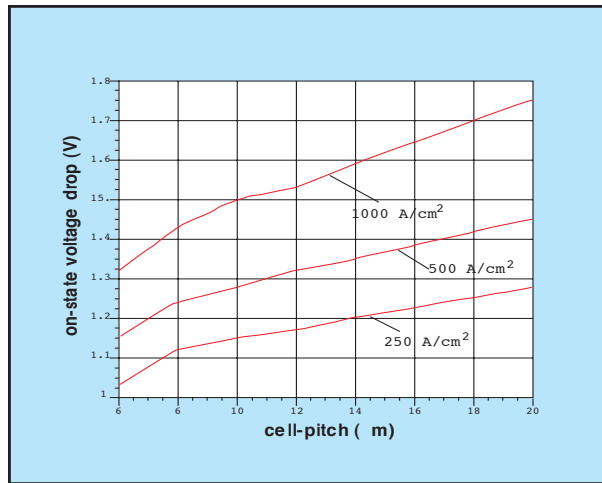


Figure 2. On-state voltage drop of a conventional TIGBT with anode density as parameters. $V_G = 15V$.

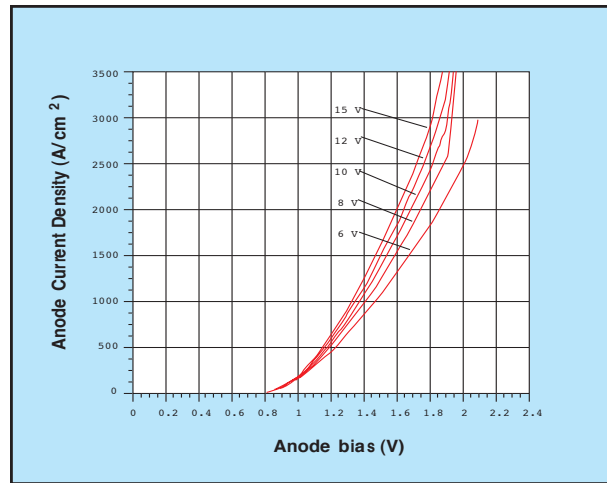


Figure 3. On-state characteristics of a conventional TIGBT. Pitch = $6\mu m$.

width per chip area results in a decrease of the channel resistance which in turn leads to higher anode current. Furthermore, even for a very small cell-pitch, no parasitic JFET-phenomenon can be observed. It is important to note, that the conventional TIGBT exhibits no saturation of the anode current for a small cell-pitch and usual gate-source voltages. However, the saturation is required to protect the device in case of short-circuit fault condition. Instead of this, a kink can be observed in Figure 3 in the anode current density. This indicates the latch-up of the parasitic thyristor structure inherent in the TIGBT. The hole current inside the p-base around the n+-region is large enough to produce a voltage drop of about $0.6V$, which forward biases the n+/p-base junction. The injected electrons flow through the n-drift region, leading to an additional hole injection from the p+-substrate which in turn increases the hole current inside the p-base. This feedback results in the loss of gate control, and the anode current continues to flow even after grounding the gate.

Resistor Diverter TIGBT

The on-state characteristic of the improved TIGBT with the diverter connected to the cathode via a resistor is shown in Figure 4 for a cell-pitch of $6\mu m$. The value of the external resistor was varied from 0 to $1000k\Omega\mu m$.

The S-shape of the current-voltage characteristics of the TIGBT with external resistor applied to the diverter can be understood as follows: Increasing the anode current slightly from zero leads to an injected hole current flowing mainly to the diverter and resulting in a low voltage drop across the resistor. This low voltage drop determines and limits the electron current which in turn limits the injection of holes and the performance of the TIGBT is rather bad. At some current level, the internal current distribution changes. The injected holes are flowing now mainly to the cathode, the injections level drastically rises, and the anode current resembles that of the conventional TIGBT.

To get a reasonable on-state behavior, i.e. a sufficiently small breakover voltage at low current levels and a sim-

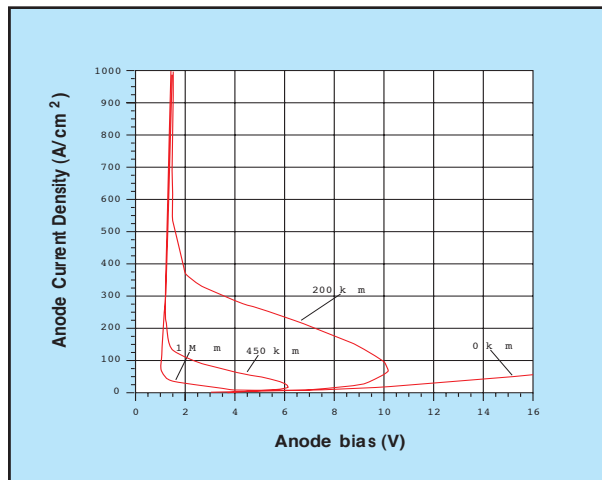


Figure 4. On-state characteristics of a resistor diverter TIGBT with varying resistance. Pitch = $6\mu m$. $V_G = 15V$.

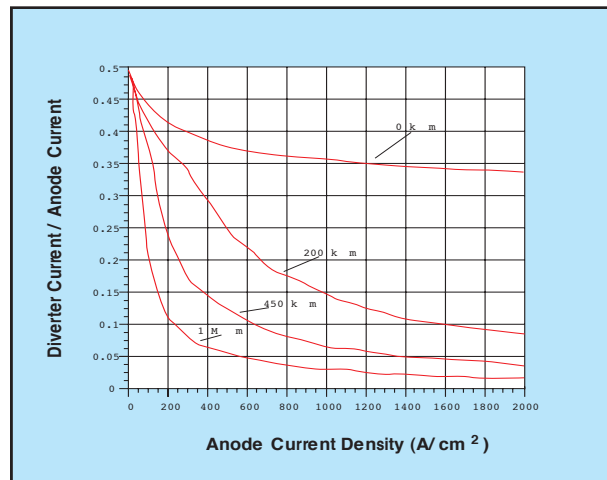


Figure 5. Ratio of diverters to anode current for a resistor diverter TIGBT with varying resistance. Pitch = $6\mu m$. $V_G = 15V$

ilar characteristic to the conventional TIGBT, it is necessary to employ a diverter resistance of $450 \text{ } \kappa\Omega\mu\text{m}$ or more. Unfortunately, a large resistance limits the value of hole-current flowing through the diverter incase of large anode currents as shown in Figure 5.

At very low anode levels the ratio of diverter to anode current exhibits a peak of about 0.5 corresponding to the situation before snapback. After snapback, the ratio decreases drastically to values below 0.05. This means that the value of the hole current flowing through the p-base is nearly the same compared to the case of the conventional TIGBT. As a result the latch-up immunity can not be improved significantly.

Another important question deals with the n-buffer surrounding the p+-diverter. The n-buffer is designed to avoid the parasitic JFET pinch-off phenomenon between the p+-diverter regions of neighbored TIGBT-cells, which would increase the on-state voltage drop of the device structure, especially for small cell-pitches. ATLAS simulation of a device with a cell-pitch of $6\mu\text{m}$ revealed, that the removal of the n-buffer yields to a S-shaped current voltage characteristic with a much higher break over voltage. This is indeed due to the JFET-effect, as the space charge region of the p+-diverter/ n-drift junction spreads far into the n-drift region and increases the resistance of the hole path through the p-base to the cathode as compared with the diverter path. However at higher current levels, after the onset of the IGBT-function, there is no significant difference in the anode currents of the devices with and without the n-buffer.

Diode Diverter TIGBT

The drawbacks of the TIGBT with resistor diverter can be circumvented by the new device structure of Figure 2B which evolved directly from the analysis in the last section. The resistor connecting the diverter with the cathode has been replaced by a pn-diode and the n-buf-

fer surrounding the p+-diverter region has been simply omitted. The non-linear current-voltage characteristic of the pn-diode leads to very promising device behavior, as seen in Figure 6. At low current densities, there exists no path through the diverter for the holes injected by the p+-substrate, and the device behaves like a conventional TIGBT. At higher current densities, when the potential inside the diverter region has been increased by a value of about 0.6V, the hole current starts to flow through the diverter instead of through the p-base.

Figure 7 shows, that the ratio of the diverter to anode current increases to a value of about 0.27. This leads to a much higher latch-up immunity of this device structure.

Furthermore, the diode lamps the potential inside the diverter region, which in turn limits the voltage drop across the inversion channel inside the MOS-part of the TIGBT. This leads to the desirable saturation-like behavior of the anode current at anode voltages beyond 2V.

Safe Operating Area

The reverse biased safe operating area (RBSOA) has been evaluated from simulations using the circuit shown in Figure 8. The diode and TIGBT were made as a single connected device structure in DevEdit allowing simulations to be run using only ATLAS. Common electrodes were defined in DevEdit to specify the connectivity.

The current source represents a snubberless inductive load, and the gate voltage is switched from 15V to 0V within 10ns. To avoid excessive computational effort, the heat transfer equation available in ATLAS/GIGA has been neglected. Instead, to take into account self-heating effects and worst case ambient temperatures, a global device temperature of 150°C was set in the simulations using the MODEL statement. Varying the clamp voltage and computing the associated maximum turn-off current density yields the RBSOA. Two physical mechanisms are responsible for the RBSOA of the TIGBT. At lower clamp

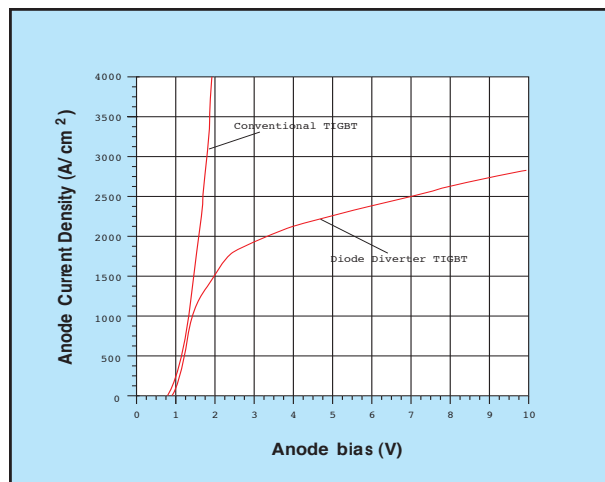


Figure 6. On-state characteristic of a diode diverters TIGBT. Pitch = $6\mu\text{m}$. $V_G = 15\text{V}$.

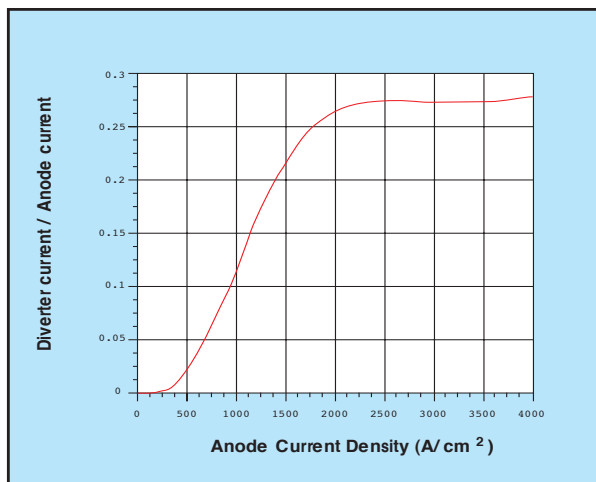


Figure 7. Ratio of diverter to anode current for a diode diverter TIGBT. Pitch = $6\mu\text{m}$. $V_G = 15\text{V}$.

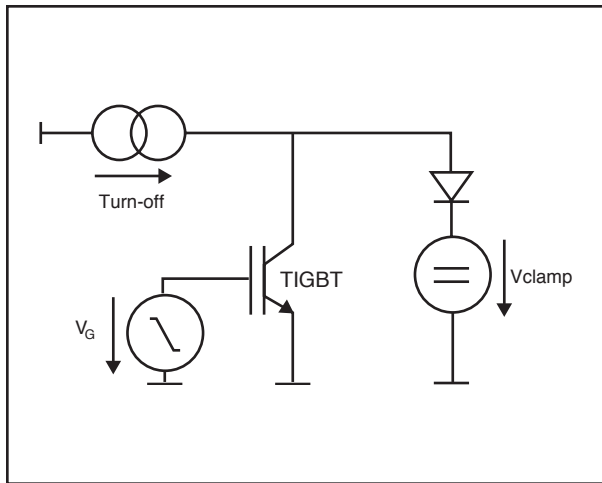


Figure 8. Circuit for RBSOA simulation.

voltages the latch-up of the inherent parasitic thyristor limits the gate-controlled current turn-off capability and at higher voltages the dynamical avalanche leads to a breakdown of the device. The dynamic latch-up current density of the conventional TIGBT at lower clamp voltages is about $1300\text{A}/\text{cm}^2$, which is roughly one third of the stationary latch-up current (Figure 9.) This can be explained as follows: After the removal of the inversion channel, the whole applied current must be carried by holes flowing into the p-base. Taking into account a typical common emitter current gain of the p+/n—drift/p-base transistor of 0.5, it is obvious that the hole current increases during inductive switching by a factor of 3, what results in a regenerative triggering of the parasitic thyristor at lower anode currents, accordingly.

In contrast, the diode diverter TIGBT exhibits a dynamic latch-up current density of about $9000\text{A}/\text{cm}^2$. The pn-diode clamps the diverter voltage near to the cathode voltage which modifies the internal potential distribution and leads to a large diverter current and a rather small hole cathode current, as shown in Figure 10. Within the first 10ns, the anode voltage increases to about 7.5V and the diverter diodes having a low differential resistance takes over the hole current. After 25ns, the anode voltage overrides the clamp voltage(100V) and the clamp diode starts to conduct the applied current. At very high clamp voltages the conventional TIGBT and the diode diverter TIGBT reveal the same RBSOA limit imposed by the dynamic avalanche.

Conclusion

All the simulated TIGBT-structures exhibit excellent on-state characteristics. The on-state voltage drop for a given current density decreases neatly linearly even for cell-pitches down to $6\mu\text{m}$. The introduction of a p+-diverter region below the trench effectively reduces the maximum electric field inside the gate-oxide to $0.1\text{MV}/$

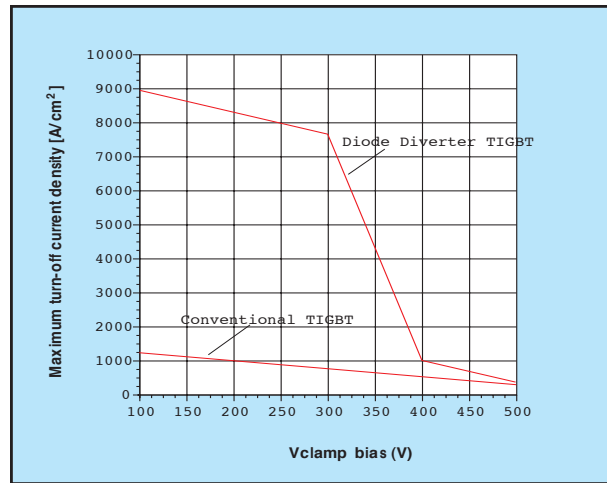


Figure 9. RBSOA of a conventional TIGBT and a diode diverters TIGBT @ 180°C .

cm at 600V blocking voltage providing increased reliability. ATLAS simulations were used to compare resistor and diode diverters to the conventional TIGBT device in terms of on-state characteristics and safe operating area. Studies of latch up immunity showed the diode diverter to be the preferred device design.

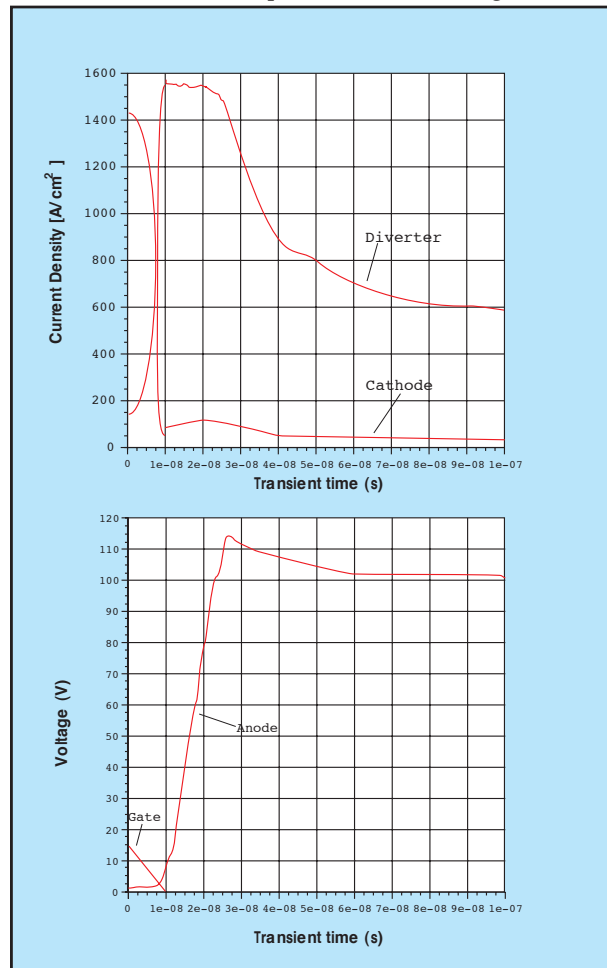


Figure 10. First phase of clamped inductive turn-off of a diode diverter TIGBT @ 150°C $I_A = 1670\text{A}/\text{cm}^2$, $V_G = 100\text{V}$.